International Journal of Astrobiology 11 (2): 71–81 (2012)
doi:10.1017/S1473550411000346 © Cambridge University Press 2011

Rotating wall vessel exposure alters protein secretion and global gene expression in *Staphylococcus aureus*

Helena Rosado[1], Alex J. O'Neill[2], Katy L. Blake[2], Meik Walther[3], Paul F. Long[4], Jason Hinds[5] and Peter W. Taylor[1]

[1]*School of Pharmacy, University College London, 29-39 Brunswick Square, London WC1N 1AC, UK*
e-mail: peter.taylor@pharmacy.ac.uk
[2]*Institute of Molecular and Cellular Biology, University of Leeds, Leeds LS2 9JT, UK*
[3]*Abteilung Genetik, Technische Universität Kaiserslautern, Postfach 3049, Paul-Ehrlich-Straße 24, 67653 Kaiserslautern, Germany*
[4]*Institute of Pharmaceutical Science, King's College, Franklin-Wilkins Building, 150 Stamford Street, London SE1 9NH, UK*
[5]*Department of Cellular and Molecular Medicine, St. George's, University of London, Cranmer Terrace, Tooting London SW17 0RE, UK*

Abstract: *Staphylococcus aureus* is routinely recovered from air and surface samples taken aboard the International Space Station (ISS) and poses a health threat to crew. As bacteria respond to the low shear forces engendered by continuous rotation conditions in a Rotating Wall Vessel (RWV) and the reduced gravitational field of near-Earth flight by altering gene expression, we examined the effect of low-shear RWV growth on protein secretion and gene expression by three *S. aureus* isolates. When cultured under 1 ***g***, the total amount of protein secreted by these strains varied up to fourfold; under continuous rotation conditions, protein secretion by all three strains was significantly reduced. Concentrations of individual proteins were differentially reduced and no evidence was found for increased lysis. These data suggest that growth under continuous rotation conditions reduces synthesis or secretion of proteins. A limited number of changes in gene expression under continuous rotation conditions were noted: in all isolates *vraX*, a gene encoding a polypeptide associated with cell wall stress, was down-regulated. A *vraX* deletion mutant of *S. aureus* SH1000 was constructed: no differences were found between SH1000 and Δ*vraX* with respect to colony phenotype, viability, protein export, antibiotic susceptibility, vancomycin kill kinetics, susceptibility to cold or heat and gene modulation. An *ab initio* protein–ligand docking simulation suggests a major binding site for β-lactam drugs such as imipenem. If such changes to the bacterial phenotype occur during spaceflight, they will compromise the capacity of staphylococci to cause systemic infection and to circumvent antibacterial chemotherapy.

Received 12 August 2011, accepted 1 November 2011, first published online 5 December 2011

Key words: bacterial microarray, continuous rotation conditions, exoproteome, *Staphylococcus aureus*, *vraX*.

Introduction

Bacteria respond to the unique environment associated with space flight. Even during short orbital flights, metabolic activity and rates of growth increase and these effects have been attributed to the influence of a low gravitational field on the external fluid dynamics surrounding cells in culture (Klaus 2002). If adaptation of bacterial pathogens to low gravity led to a more pathogenic phenotype, it could jeopardize extended space flight, particularly as it is well documented that deleterious changes to the human microbiota and the immune status of crew occur following prolonged periods aboard space vessels (Taylor 1974; Sonnenfeld & Shearer 2002; Taylor & Rosado 2007). Although controversial (Taylor & Rosado 2007), experiments undertaken aboard Earth orbiters indicate that Gram-positive and Gram-negative bacteria become reversibly less susceptible to a range of antibiotics compared with ground-based controls (Lapchine *et al*. 1985; Tixador *et al*. 1985). There are also reports that space flight enhances the virulence of Gram-negative pathogens (Wilson *et al*. 2007, 2008).

As opportunities to examine the effects of space flight on bacterial phenotypes arise only infrequently and are limited by the constraints of in-flight experimentation, ground-based bioreactors have been developed to replicate the low fluid shear culture conditions that occur in microgravity. In particular, the High Aspect Rotating Vessel (HARV; Hammond & Hammond 2001) has stimulated a considerable amount of research into the effect of low-shear continuous rotation (LSCR) conditions on the physiology of a wide range of cells, including bacteria. In an extensive series of investigations of the effect of LSCR on the phenotype of *Salmonella enterica* Serovar Typhimurium, Nickerson and co-workers provided evidence that LSCR acts as an environmental signal for

https://doi.org/10.1017/S1473550411000346 Published online by Cambridge University Press

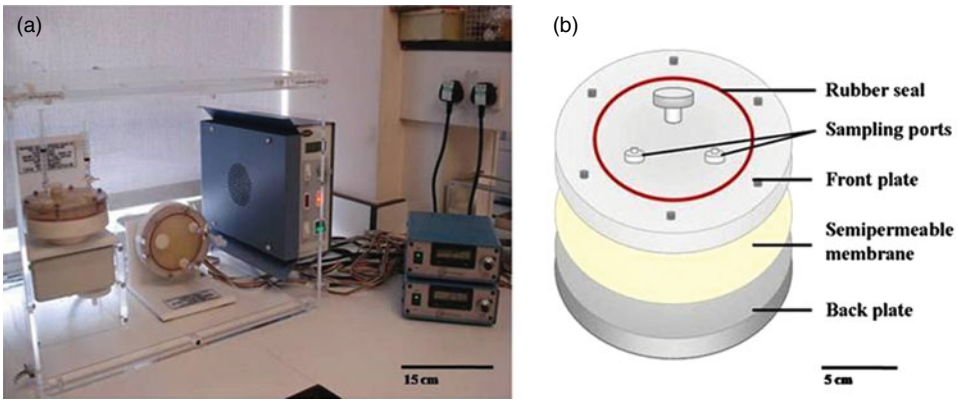


Fig. 1. The rotary cell culture system. (a) Laboratory experiment setup showing the 50 ml culture vessel in both the LSCR (rotation about the horizontal axis) and 1 ***g*** (rotation about the vertical axis) orientation; (b) elements of the HARV. Samples were loaded through a port in the HARV; dimensions of the HARV and ancillary apparatus are shown.

expression of enhanced bacterial virulence in this organism. LSCR-grown cells produced a shortened time to death of infected mice and more readily colonized in liver and spleen compared with normal gravity (1 ***g***) controls (Nickerson *et al.* 2000a,b, 2004). The expression of over 160 *S. typhimurium* genes encoding functionally diverse proteins was differentially regulated under LSCR (Wilson *et al.* 2002) and a similar transcriptomic pattern was induced by space flight (Wilson *et al.* 2007).

However, the risk posed by this gastrointestinal pathogen is likely to be small in comparison with the potential threat of infection due to opportunistic bacteria originating from the microbiota of members of the flight crew. Regular monitoring of air, water and surfaces inside the International Space Station (ISS) has indicated that by far the most prominent contaminants are staphylococci, with *Staphylococcus aureus* frequently encountered (Novikova 2004; Novikova *et al.* 2006). Infection of open wounds, likely to occur on extended missions, with *S. aureus* would threaten not only the future of the mission but also the immediate wellbeing of the crew member, a situation that would be exacerbated by any gravity-induced increases in antibiotic resistance. *S. aureus* has been flown in space only twice, aboard Salyut 7 (Tixador *et al.* 1985) and Mir (Juergensmeyer *et al.* 1999), for the investigation of the effects of space flight on antibiotic susceptibility, with inconclusive results. Under LSCR, no differences were found in gross bacterial morphology or susceptibility to the antibiotics erythromycin, flucloxacillin and vancomycin of HARV-grown nosocomial isolates of *S. aureus* compared with growth under 1 ***g***, but some evidence was obtained for LSCR-mediated modulation of factors associated with staphylococcal virulence (Taylor & Rosado 2007). To investigate the impact of growth under LSCR conditions on the staphylococcal phenotype in relation to the expression of determinants of virulence, we have undertaken an investigation of protein secretion and gene expression in three antibiotic-susceptible isolates selected for their phenotypic diversity (Taylor & Rosado 2007) and grown under LSCR and 1 ***g***. *S. aureus* relies on a repertoire of secreted or surface-located adhesins, invasins and toxins to invade and damage the host (Novick 2003).

Materials and methods

Bacteria and growth conditions

The methicillin susceptible *S. aureus* (MSSA) isolates RF1, RF6 and RF11 were obtained from the Royal Free Hospital, London, UK. These non-motile isolates were selected for study on the basis of differences in colony size, pigmentation and haemolysin production following culture on sheep blood agar.

Bacteria were grown in Müller–Hinton (MH) broth (Oxoid) using 50 ml Synthecon RCCS-1 HARVs (Cellon SA, Bereldange, Luxembourg) housed in a 37 °C incubator. The experimental set-up and details of the culture vessel are shown in Fig. 1. Shake flask MH broth cultures were incubated for 16 hours at 37 °C, diluted 1:50 in fresh MH broth and transferred into the bioreactor compartment. The bioreactors were then orientated to grow cells under conditions of LSCR (rotation about the horizontal axis) or 1 ***g*** (rotation about the vertical axis). In all experiments, LSCR and 1 ***g*** cultures were grown simultaneously with a rotation rate of 25 rpm for up to 24 hours. Mathematical modelling has indicated that the fluid shear level within the vessel is less than 1 dyne/cm^3 (Nauman *et al.* 2007). It has been shown by Schwartz *et al.* (1992) that under these conditions the simulated gravitational field for horizontally rotated cultures is equivalent to 0.01 ***g***.

Lysis of bacteria in HARV culture was monitored by scanning electron microscopy (SEM) and transmission electron microscopy (TEM) and by determination of DNA in culture supernatants by electrophoresis using 1% agarose gels containing 0.5 μg/ml ethidium bromide. DNA was precipitated from unit volumes of supernatant (normalized on the basis of cell dry weight) with 3 M sodium acetate, pH 5.2, and with absolute ethanol; after separation DNA was visualized by exposure to ultraviolet light, quantified by scanning with a Molecular Imager Fx (BioRad) and with a NanoDrop

https://doi.org/10.1017/S1473550411000346 Published online by Cambridge University Press

spectrophotometer and compared with samples obtained from cultures of the corresponding strain treated with Lysing Matrix B (Qbiogene).

Generation of vraX deletion strain

Established procedures (Bae & Schneewind 2006) were used to delete the entire *vraX* gene from the chromosome of *S. aureus* SH1000 (Horsburgh *et al*. 2002; O'Neill 2010). Briefly, two DNA fragments, corresponding to the up- and down-stream flanking regions of the *vraX* gene, were amplified by polymerase chain reaction (PCR) using oligonucleotide primer pairs GGGGACAAGTTTGTACAAAAAAGCAGGCTAGGCGCACAGCATGTCATCATTAAAGGTGG/TATATTGGATCCTTTGCTACTCTATGGTTA and TAGGGATCCTGACTAATCGTTCCAATAATC/GGGGACCACTTTGTACAAGAAAGCTGGGTTTTATTATTTAAAGATGGTGTTACGGTAGG (engineered regions underlined). Following purification and digestion with *Bam*HI, equimolar amounts of these amplicons were ligated together and recombined into plasmid pKOR1 for transformation into *Escherichia coli* DH5α (Bae & Schneewind 2006). The resulting construct was verified by DNA sequencing, electroporated first into the restriction-deficient host *S. aureus* RN4220, and then recovered and electroporated into *S. aureus* SH1000. The *vraX* gene was subsequently deleted from the chromosome of SH1000 by allelic replacement (Bae & Schneewind 2006). Successful deletion of *vraX* was confirmed by PCR amplification and DNA sequencing of a 6 kb fragment encompassing the *vraX* locus.

Protein extraction

For preparation of extracellular protein extracts from 50 ml batches of bacterial suspensions, culture supernatants were filtered (0.22 µm) and supernatant proteins concentrated 30-fold using Vivaspin 20 ultrafiltration spin columns (Sartorius). For preparation of cell protein extracts, bacteria were washed twice with ice-cold TE sample buffer (10 mM Tris/HCl and 1 mM EDTA, pH 8.0), and suspended in ice-cold base sample buffer (7 M urea, 2 M thiourea and 4% CHAPS, Roche protease cocktail tablet). The cells were disrupted by homogenization with glass beads in a FastPrep (Qbiogene) for 40 seconds at 6.0 m/s. Lysates were centrifuged to remove cellular debris, followed by centrifugation at 21 000 ***g*** for 45 minutes at 4 °C to remove insoluble proteins. Protein concentration was determined by Bradford assay and protein samples prepared for IEF using a 2D clean-up kit (BioRad).

Protein gel electrophoresis

2D gel electrophoresis (2DE) was performed using a Protean IEF Cell (BioRad). Proteins were separated with 17 cm immobilized pH gradient strips (BioRad) and pH range 4–7. The strips were allowed to rehydrate for 12 hours under mineral oil. Voltage was increased by gradient from 250 to 10 000 V for 2 hours with a final phase of 10 000 V for 80 000 Vh. The strips were equilibrated first in dithiothreitol (DTT) and then in iodoacetamide, both for 15 minutes. For identification of proteins by Matrix-assisted laser desorption/ionisation time of flight mass spectrometry (MALDI-TOF-MS), 300 µg of cellular and extracellular proteins was separated using preparative 2D gels. SDS-PAGE was performed with 12% polyacrylamide gels and proteins stained with Sypro Ruby or CBB R-250. Gels were scanned with a Molecular Imager Fx (BioRad), and processed by PDQuest Advanced 2D-image analysis software (BioRad). At least three biological replicates were performed for each experiment and proteins showing at least a twofold change ($P \leqslant 0.05$) were considered to be significantly modulated.

Protein identification

Proteins were identified by MALDI-TOF-MS or MALDI-TOF-MS/MS. CBB-stained protein spots were cut from gels using an EXQuest spot cutter (BioRad) fitted with a picker head of 1.5 mm and transferred into a 96-well microtitre plate. The plate was loaded onto a MassPrep robotic liquid handling system (Waters/BioRad Proteome Works) to destain the gel pieces, reduce and alkylate cysteine residues using DTT and iodoacetamide, carry out in-gel tryptic digestion and extract the resulting peptide mixture into a 96-well PCR plate. The extracted peptide mixture was manually desalted using C18 loaded zip-tips (Millipore) and 2 µl spotted onto sample wells of a stainless steel MALDI target plate that had been previously spotted with 1 µl of matrix solution comprising 1 mg/ml α cyano-4-hydroxycinnaminic acid (Sigma) in 50% acetonitrile, 50% ethanol and an internal standard, adenocorticotrophic hormone (ACTH; Sigma), at a final concentration of approximately 100 fmol/µl in 0.1% formic acid. Air-dried samples were analysed using a Waters MALDI-TOF-MS operating at a resolution of >10 000 full-width at half-maximum in reflectron mode. Spectra (λ_{337}) were acquired at 5 Hz using a nitrogen laser. Typically, ten data collection events were combined to generate each spectrum. Data acquisition were achieved by random sampling from the target well. Peptide peak-list files were generated manually. Background peaks observed in blank gel control samples resulting from trypsin autolysis and commonly observed keratin contamination was excluded from database searching. Peak lists were entered into a MASCOT PMF database search engine; search parameters included a peptide mass accuracy tolerance of 0.2 Da and searches allowed for modifications such as alkylation of cysteine during the tryptic digest procedure and the formation of methionine sulfoxide.

Microarray analysis

The BµG@S SAv1.1.0 microarray has been described elsewhere (Witney *et al*. 2005) and contains PCR products representing all predicted open reading frames from the initial seven *S. aureus* genome sequencing projects. The array design is available from the website BµG@Sbase (accession number: A-BUGS-17; http://bugs.sgul.ac.uk/A-BUGS-17) and also ArrayExpress (accession number: A-BUGS-17). For preparation of total RNA, 50 ml aliquots of bacterial suspensions were harvested by centrifugation, the cells suspended in 1 ml of RNA protect Bacteria reagent (Qiagen) and incubated for 5 minutes at room temperature. Samples were then centrifuged

https://doi.org/10.1017/S1473550411000346 Published online by Cambridge University Press

Table 1. *Oligonucleotide primers for qRT-PCR*

Gene	Forward primer	Reverse primer
16 s rRNA	ACTGAGACACGGTCCAGACT	CGGATAACGCTTGCCACCTA
hla	CTGTCGCTAATGCCGCAGAT	AAGGCTGAAGGCCAGGCTAA
saeRS	TGCCAACCATTGGAGCAACG	GCCAATACCTCCATCGCTAA
gapA2	GCTAGTTATCCACCCGAAAC	GGCAAGCTTTCAGGATTACG
clpL	CTTAACCGCTTCAACGGCAT	GCGTGCGCCTAATTCTTCAT
dnaK	CCTACACGCCAAGCAATGAA	GTGATAACGCCACCTTGGAT
sarA	ACATGGCAATTACAAAAATCAATGAT	TCTTTCTCTTTGTTTTCGCTGATG
sigB	CGATGAACTAACCGCTGAAT	GCGTAACAGTTGAACCATCT

(10 minutes; 4 °C; 3000 ***g***), pellets frozen on dry-ice and maintained at −80 °C. Total RNA was isolated using FastRNA® Pro Blue kit (Qbiogene) and treated with DNase I using RNase-Free DNase set protocol and RNeasy minikit protocol (Qiagen). Total RNA was quantified with a NanoDrop spectrophotometer and 5 µg aliquots labelled with Cy5 or Cy3 dye (GE Healthcare) concomitant with reverse transcription into cDNA using SuperScript™ II reverse transcriptase (Invitrogen). Labelled cDNA was then purified using a MinElute kit (Qiagen), the probes pooled, hybridized overnight to the *S. aureus* microarray at 65 °C and subjected to stringent washing (Witney *et al*. 2005). Hybridization data were acquired using an Affymetrix 428 scanner quantified using Bluefuse for Microarrays 3.5 software (BlueGnome). Data analysis was performed in GeneSpring GX 7.3 (Agilent) using median-normalized Cy5/Cy3 ratio intensities for three biological replicates. Only genes whose expression ratio showed at least a twofold difference with Benjamini and Hochberg false discovery rate $\leqslant 0.05\%$ under LSCR were regarded as being significantly different from the control. Fully annotated microarray data have been deposited in BµG@Sbase (accession number E-BUGS-113 http://bugs.sgul.ac.uk/E-BUGS-113) and ArrayExpress (accession number E-BUGS-113).

Quantitative real-time PCR (qRT-PCR)

qRT-PCR was carried out using the Brilliant II SYBR® Green qRT-PCR 1-Step kit (Stratagene); 50 ng of DNA-free RNA was used as template for cDNA synthesis and the cDNA obtained was used for each PCR reaction. Gene-specific primer pairs were designed for genes of interest to yield amplicons of 100–150 bp. The conditions for the PCR were: 95 °C for 10 minutes, followed by 55 cycles of 95 °C for 30 seconds, 55 °C for 30 seconds and 72 °C for 30 seconds. The comparative threshold method was used to determine relative quantification of mRNA abundance and changes in mRNA expression level were calculated after normalization to the internal control, 16S rRNA. The nucleotide sequences of the primers used in this study are presented in Table 1.

In silico modelling

An *ab initio* structural prediction for the VraX protein (accession number NP_371103) was performed using the Rosetta 3.1 program package (Leaver-Fay *et al*. 2011). Rosetta uses a fragment assembly method with a Monte Carlo simulated annealing algorithm to build up the tertiary structure out of the primary sequence (Rohl *et al*. 2004). In the first step, 10 000 VraX structures were generated and the 500 with the best Rosetta score were clustered into groups according to their backbone similarity. Representatives of each cluster were used for structure refinement and the structure with the best Rosetta score was used for protein–ligand docking using AutoDock4.2 (Morris *et al*. 2009). The β-lactam drug imipenem was used as a representative β-lactam ligand. During the docking, the VraX protein was treated as a rigid body and imipenem was allowed full flexibility around the rotatable bonds.

Results

Growth under LSCR reduces protein secretion by S. aureus

The growth kinetics, final cell mass (determined as cell dry weight) and antibiotic susceptibility of *S. aureus* RF1, RF6 and RF11 were essentially identical after 24 hours HARV culture, when OD_{600} was approximately 2, under 1 ***g*** and LSCR conditions (Taylor & Rosado 2007). There was no evidence of a shortened lag phase and increased final cell count, as has been recorded with other non-motile bacteria (Benoit & Klaus 2007). However, at this time point, significantly less protein was found in the growth medium of LSCR cultures of these isolates in comparison with 1 ***g*** cultures (Fig. 2). There were large variations between strains in the amount of extracellular protein (the exoproteome) associated with 1 ***g*** grown cells, with isolate RF6 secreting twice the amount compared with RF1 and four times that of RF11, but under LSCR all three isolates released comparable amounts of protein into the surrounding medium (0.04–0.05 mg protein/mg dry cell mass). Culture under LSCR conditions reduced the amount of exoprotein by a factor of 2.0 for RF1, 5.5 for RF6 and 1.2 for RF11 (Fig. 2). Growth kinetics, final cell mass, antibiotic susceptibility and protein secretion profiles of RF1, RF6 and RF11 grown under 1 ***g*** were essentially identical to those found when the bacteria were grown for 24 hours in 50 ml shake flask cultures (200 orbits/minute).

2DE was undertaken to monitor the impact of LSCR on the profile of the exoproteome. The secreted protein profiles of RF1, RF6 and RF11 were comparable and >300 individual spots were resolved for each isolate. With all three isolates, the exoprotein profile was substantially altered by LSCR and a large number of proteins were present in the growth medium in

https://doi.org/10.1017/S1473550411000346 Published online by Cambridge University Press

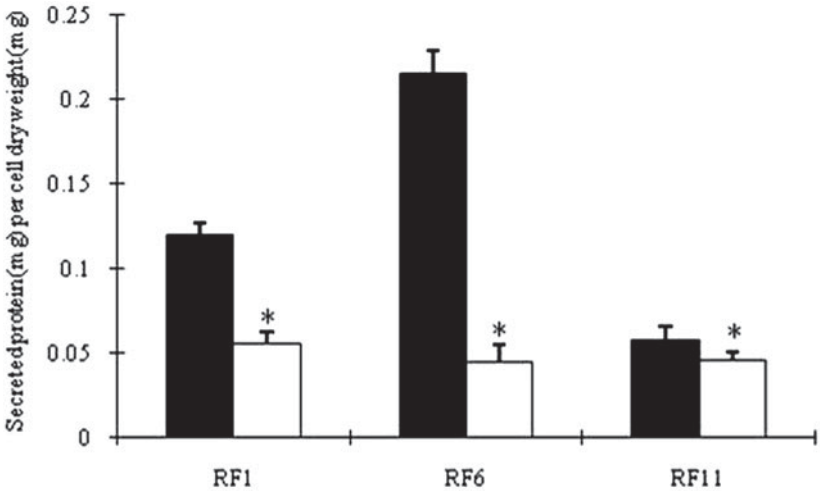


Fig. 2. Total protein secreted by *S. aureus* RF1, RF6 and RF11 following 24 hours growth in the HARV under 1 ***g*** (■) and LSCR (□), expressed as protein concentration (mg) per unit mass (mg) of bacterial dry weight. At the sampling time point, cells were in early stationary phase, OD_{600} approximately 2 (Jones *et al.* 2008). Error bars represent 1 SD; $n = 5$; *significant ($P < 0.0001$) using paired, two-tailed Student's *t* test.

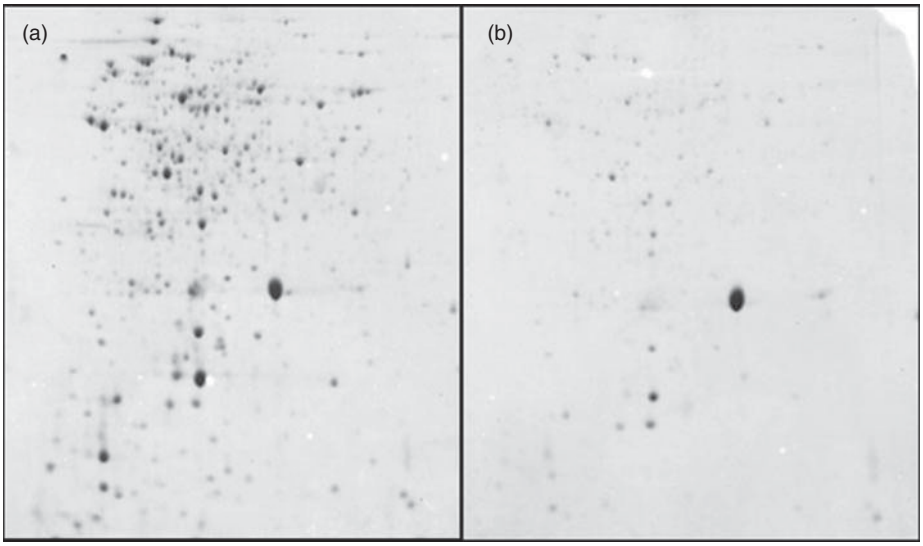


Fig. 3. 2DE of soluble proteins in the culture supernatant of *S. aureus* RF6 grown under 1 ***g*** (a) and LSCR (b). The quantity loaded onto the gel (A: 300 µg; B: 54.5 µg) corresponded to the total protein complement secreted by a unit of cell dry weight. Proteins were visualized with CBB.

reduced amounts. This was particularly apparent with RF6 (Fig. 3), the isolate showing the largest decrease in extracellular protein under LSCR. 2DE exoproteome profiles for the three isolates grown under 1 ***g*** were comparable and the 51 most prominent proteins associated with the exoproteome of RF6 were identified by MALDI-TOF-MS of peptide mass fingerprints. LSCR-induced changes to the exoproteome, reduced the concentration of some proteins to a level below the detection limit if the protein complement secreted by a unit of cell dry weight was applied to the gel. In order to compare the exoproteome from 1 ***g***- and LSCR-grown bacteria, a standardized quantity (300 µg) of protein was applied to each gel, fluorescence intensity determined and the relative concentrations per unit cell dry weight then calculated.

Quantitative differences in the most abundant components of the exoproteome of RF1, RF6 and RF11, grouped with respect to protein function, are shown in Table 2; as has been noted by others (Ziebandt *et al.* 2001, 2004; Tjalsma *et al.* 2004; Sibbald *et al.* 2006), many proteins found in the extracellular milieu can be ascribed typical cytoplasmic functions. The most abundant protein in the exoproteome, immunodominant staphylococcal antigen A (IsaA), was relatively unaffected by growth under LSCR. In contrast, proteins associated with protein synthesis, folding and degradation, glycolysis, oxidative phosphorylation and various catabolic and metabolic functions were markedly reduced in the exoproteome of RF6, and variably reduced in the case of the isolates RF1 and RF11 (Table 2). To determine

https://doi.org/10.1017/S1473550411000346 Published online by Cambridge University Press

Table 2. *Relative fluorescence intensities of the most abundant proteins from the exoproteome of* S. aureus *RF1, RF6 and RF11 in 2DE following growth under LSCR, compared with 1 **g***

Function		Protein name	Mean-fold change		
			RF1	RF6	RF11
Protein synthesis, folding and degradation					
1[a]	Dps	General stress protein 20U	−1.81	−16.23**	−1.45*
7	TufA	Translational elongation factor Tu	−3.54	−24.88**	−1.07
23	RpsA	30S ribosomal protein S1	−2.73*	−31.69**	1.49*
36	Tig	Trigger factor prolyl isomerase	−2.25	−32.32**	1.04
37	GroEL	60 kDa chaperonin	–[b]	−21.80*	–
39	DnaK	Chaperone protein	−1.87	−39.64*	1.06
40	ClpL	Putative ATP-dependent Clp proteinase, proteolytic subunit ClpL	−2.09	−25.52	1.01
42	EF-G/FusA	Elongation factor G	−3.62*	−33.46*	1.93
48	HchA	Chaperone protein hchA (Hsp31)	–	−15.02**	1.06
49	EF-T/Tsf	Translation elongation factor Ts	−1.64	−14.75**	−2.10*
Glycolysis					
8	Fba	Fructose-bisphosphate aldolase	–	−10.33*	–
11	PdhB	Pyruvate dehydrogenase E1 component beta subunit	−1.80	−25.84**	−1.93**
15	Gap	Glyceraldehyde-3-phosphate dehydrogenase, type I	−1.59	−59.46*	−1.58
24	Eno	Phosphopyruvate hydratase – Enolase	−3.99**	−24.75**	−2.78**
38	PtsI	Phosphoenolpyruvate-protein phosphotransferase	–	−19.43**	–
51	Pgk	Phosphoglycerate kinase	−1.77	−19.14*	1.07
Tricarboxylic acid cycle					
10	SucD	Succinyl-CoA ligase (ADP-forming) subunit α	−1.20	−45.53**	−1.01
13	CitC	Isocitrate dehydrogenase (NADP)	−4.09*	−68.39*	–
19	CitZ	Citrate synthase II	−17.90**	−322.82*	−1.61**
43	CitB	Aconitate hydratase I	−2.59	−33.99*	−1.75
Oxidative stress					
5	SodA	Superoxide dismutase	−2.43*	−13.59**	−2.65**
25	AldA	Putative aldehyde dehydrogenase	–	−26.73**	–
29	KatA	Catalase	−13.83**	−36.09**	−2.16**
Amino acid synthesis					
9	CysK	Cysteine synthase	−2.95*	−21.49*	−1.13
17	ACOAT2	Acetylornithine aminotransferase 2	−1.47	−39.93*	−2.55
27	GlnA	Glutamine synthetase, type I	−2.84	−31.20**	−2.30
Carbon metabolism					
22	GlyA	Serine hydroxymethyltransferase	−4.22	−25.82**	–
31	Fhs	Formate-tetrahydrofolate ligase	−4.91*	−53.46**	−2.37*
Acetate metabolism					
21	AckA	Acetate kinase	−1.79	−49.41**	−2.35*
32	PdhD	Dihydrolipoamide dehydrogenase component of pyruvate dehydrogenase E3	−2.55**	−22.46**	−1.95
Pyrimidine metabolism					
14	PYNP	Pyrimidine nucleoside phosphorylase	−4.64**	−35.98**	–
Iron transport and storage					
2	FtnA	Ferritin	−1.52*	−10.02	1.18
Unconfirmed function					
3	Asp23	Alkaline shock protein	−1.95	−8.95	1.06*
6	IsaA	Immunodominant antigen A	1.16*	1.68*	2.53**
12	PpaC	Probable manganese-dependent inorganic pyrophosphatase	−4.42	−22.49**	−1.44

Proteins identified by LC/MS-MS.; $n = 3$; $^{*}P < 0.05$, $^{**}P < 0.01$.
[a] Reference number on 2D master gel.
[b] Protein not detected.

whether changes in the abundance of these proteins were due to a reduction in cell lysis induced under conditions of LSCR, DNA associated with the 24 hours growth medium was quantified after separation on agarose gels containing ethidium bromide. Lysed (control) bacteria from HARV cultures of the three isolates produced intense, broad bands under UV light; no DNA was detectable in supernatants from any 1 ***g***- and LSCR-grown samples unless the samples were concentrated at least 30-fold. The degree of lysis was calculated to be less than 0.01%.

https://doi.org/10.1017/S1473550411000346 Published online by Cambridge University Press

Table 3. *Genes with altered expression following growth of* S. aureus *RF1, RF6 and RF11 under LSCR, compared with 1 **g***[a]

Isolate	Genes/open reading frames	Description	Mean-fold change[b]
RF1	SAR1545	Hypothetical phage protein	5.52
	gap2	Glyceraldehyde 3-phosphate dehydrogenase 2	4.95
	SAR1150	Antibacterial protein	2.86
	SAR1370	Hypothetical protein	2.83
	SAR2264	Conserved hypothetical protein	2.80
	SAV0855	Hypothetical protein	2.79
	clpL	ATP-dependent protease ATP-binding subunit ClpL	2.51
	hutU	Urocanate hydratase	2.49
	narT	Nitrite transport protein	2.48
	blaZ	β-lactamase precursor	2.44
	SAR2096	Putative anti repressor	2.34
	COL2004	–	2.33
	SAR0624	Putative esterase	2.11
	SAR1459	Conserved hypothetical protein	2.10
	SAR1458	Conserved hypothetical protein	2.09
	SAV0912	Hypothetical protein	−3.75
	nuc	Thermonuclease precursor	−2.98
	SAR2001	Staphopain protease	−2.85
	SAR0189	Putative thiamine pyrophosphate enzyme	−2.75
	SAR0435	Exotoxin	−2.28
	vraX	Predicted role in imipenem resistance	−2.23
	SAR0390	Putative lipoprotein	−2.13
	hsdS	–	−2.09
	SAR1266	Conserved hypothetical protein	−2.09
	SAR0583	Hypothetical protein	−2.06
RF6	*gapA2*	Glyceraldehyde 3-phosphate dehydrogenase 2	2.94
	COL3568	–	2.14
	hla	α-haemolysin precursor (pseudogene)	−5.25
	vraX	Predicted role in imipenem resistance	−4.53
	SAR1651	Putative membrane protein	−2.56
	SAR0279	Conserved hypothetical protein	−2.39
	saeS	Histidine kinase protein	−2.37
	saeR	Response regulator protein	−2.34
	fadD	Putative acyl-CoA dehydrogenase	−2.31
	geh	Lipase precursor	−2.11
	SAR0760	Putative membrane protein	−2.07
	SAN2285	Putative cell wall-anchored protein	−2.01
RF11	*clpL*	ATP-dependent protease ATP-binding subunit ClpL	2.43
	SAR0217	Formate acetyltransferase	2.20
	dnaK	Chaperone protein	−3.13
	vraX	Predicted role in imipenem resistance	−2.41

[a] Refer to Rosado *et al.* (2010).
[b] Changes in gene expression shown as mean-fold change for LSCR grown compared with 1 ***g*** grown cells (LSCR/1 ***g***); $P < 0.05$.

The intracellular proteome of the three isolates following 24 hours growth was also examined by comparing 1 ***g*** and LSCR cultures; significant ($P < 0.05$) differences in concentration were found with only five proteins.

S. aureus *gene expression responds to LSCR*

A preliminary assessment of the microarray data was presented by Rosado *et al.* (2010) and is described here in detail. The three isolates (RF1, RF6 and RF11) were selected for investigation on the basis of differences in their phenotypes and this was reflected in the distinctive patterns of gene expression found for each strain under each set of growth conditions. In a similar fashion, each strain responded in a different manner to growth under LSCR (Table 3). Significant changes in gene expression of 25 genes were found with RF1; 15 were up-regulated greater than 2-fold and ten down-regulated at least 2-fold. In contrast, only two genes were significantly up-regulated in the case of RF6 but ten were down-regulated. The degree of significant gene modulation was minimal with RF11, with two genes up-regulated and two down-regulated. No evidence was found for coordinated modulation of genes within operons. Glyceraldehyde 3-phosphate dehydrogenase 2 (*gapA2*) was up-regulated greater than 2-fold in RF1 and RF6 and putative ATP-dependent protease ATP-binding subunit ClpL (*clpL*) was significantly up-regulated in RF1 and RF11. Levels of up-regulation of both *gapA2* and *clpL* were significant in all three isolates when gene expression was analysed using qRT-PCR (Table 4). One gene, *vraX*, encoding a small (55 amino acids) polypeptide previously found to be up-regulated following emergence of vancomycin intermediate-resistance in sequential isolates of *S. aureus* (McAleese *et al.* 2006), during experimental *S. aureus* infections (Scherl *et al.* 2006), following exposure to cell wall-active antibiotics including vancomycin (Utaida *et al.* 2003; McAleese *et al.* 2006) and the cell membrane-active agents daptomycin (Muthaiyan *et al.* 2008) and epicatechin gallate (Bernal *et al.* 2010), was down-regulated under LSCR in all three isolates. We therefore deleted in its entirety the *vraX* gene from laboratory strain *S. aureus* SH1000. This strain was selected as, unlike isolates RF1, RF6 and RF11, its genome has been sequenced in its entirety and characterized, and the strain is well established as suitable for genetic manipulation. No differences were detected in the growth rate, viability or susceptibility to sub-inhibitory and supra-inhibitory concentrations of vancomycin (a potent inducer of *vraX*; approximately 100-fold in this study) of Δ*vraX* compared with the parent strain. The mutant and wild-type showed no differences in susceptibility to the antibiotics oxacillin, vancomycin, erythromycin and mitomycin C as determined by Minimum inhibitory concentration (MIC). Similarly, no differences were found between mutant and wild-type with respect to pigment production and erythrocyte lysis observed after overnight culture on 3% sheep blood agar or with regard to their sensitivity to overnight incubation at 30 and 42 °C. Most importantly, no qualitative or quantitative differences in protein recovered from supernatants after 8, 16, 18 and 24 hours growth were detected using SDS-PAGE gels. Comparison of mid-logarithmic phase broth cultures using the BμG@S SAv1.1.0 microarray revealed no significant changes in gene expression other than loss of *vraX* expression in the mutant; induction with 2 μg/ml vancomycin elicited an essentially identical gene expression response (*vraX* excepted) in the mutant compared with the wild strain (http://bugs.sgul.ac.uk/E-BUGS-113).

An *ab initio* structural prediction for VraX showed a very compact structure with β-sheets and one α-helix (Fig. 4(a)). The

https://doi.org/10.1017/S1473550411000346 Published online by Cambridge University Press

Table 4. *Validation by qRT-PCR of microarray data for* S. aureus *RF1, RF6 and RF11*

		Mean-fold change[a]	
Gene	Isolate	Microarrays	qRT-PCR
hla	RF1	−1.35	−2.17**
	RF6	−5.26*	−6.67*
	RF11	1.18	1.15
saeR/S	RF1	1.03	−2.94*
	RF6	−2.38*	−5.56*
	RF11	−1.05	−1.02
gapA2	RF1	4.95*	7.66**
	RF6	2.94*	9.49**
	RF11	1.34	6.20**
clpL	RF1	2.52*	2.43*
	RF6	1.23	2.73*
	RF11	2.43*	4.40*
dnaK	RF1	1.39	−1.37
	RF6	1.41	1.09
	RF11	−3.13*	−3.57*
RNAIII	RF1	–	
	RF6	–	
	RF11	–	
sarA	RF1	–	−1.33*
	RF6	–	1.38
	RF11	–	1.76
sigB	RF1	–	−1.47
	RF6	–	−1.59
	RF11	–	1.12

[a]Changes in gene expression shown as mean-fold change for LSCR-grown cells compared with 1 ***g***-grown cells. *$P<0.05$; **$P<0.01$.

β-sheets form a plane and the α-helix is located above and across this plane. Using the VraX amino acid sequence as a seed for BLAST searching the NCBI non-redundant protein database (http://blast.ncbi.nlm.nih.gov/Blast.cgi) indicated that VraX was restricted to staphylococci, in many cases as an uncharacterized protein, but with no significant hits to any other proteins in any other organisms. A multiple sequence alignment of staphylococcal VraX amino acid sequences revealed the conserved motif LLSLL. The conserved serine is located in the α-helix and should be accessible for chemical reactions. The protein–ligand docking suggests that a major binding site for imipenem is close to this serine (Fig. 4(b)).

The highest reduction in protein export under LSCR was seen with RF6 (Fig. 3) and in this strain the α-toxin gene *hla* was down-regulated greater than 5-fold; *hla* is partially regulated by the two-component signal transduction system SaeRS (Giraudo *et al*. 1997; Novick & Jiang 2003) and down-regulation by LSCR of *saeR* and *saeS* in RF6 also reached levels of statistical significance (Table 3). Microarray data indicated that expression of *hla, saeR* and *saeS* was reduced in strains RF1 and RF11 but did not reach levels of statistical significance. Expression of these genes were therefore investigated using qRT–PCR and the data provided further evidence for down-regulation in RF1 and RF11 (Table 4). There was excellent correlation between microarray and qRT-PCR data with genes selected for qRT-PCR validation (Table 4).

Discussion

A number of studies have provided evidence that both the spaceflight environment and ground-based simulations alter the properties of bacteria in a way that may impact on their capacity to establish infectious foci and persist at the infected site, with clear ramifications for extended manned space flight. Apparent small decreases in the susceptibility of *E. coli* and *S. aureus* to a range of antibiotics after cultivation aboard the Earth orbiter Salyut 7 (Lapchine *et al*. 1985; Tixador *et al*. 1985) have implications for the treatment of bacterial infections that may arise if and when planned missions to Mars take place, particularly in view of emerging evidence that drug formulations are less stable during space flight (Du *et al*. 2011). If changes in the expression of *S. enterica* genes considered to confer increased virulence under LSCR (Wilson *et al*. 2002) and during short-term space flight (Wilson *et al*. 2007) occurred in bacterial pathogens likely to be found as components of the microbiota of the crew, this could result in an increased incidence of intractable infection during extended flight (Taylor & Rosado 2007). To investigate these issues, we examined the antibiotic susceptibility and gross morphology under LSCR of drug-sensitive isolates of *S. aureus*, an opportunistic pathogen with the potential to cause serious infections, particularly in individuals with reduced immune function, a state found with high frequency among astronauts during and immediately following space flight (Sonnenfeld 2005). There were no differences in the antibiotic susceptibility profiles of 1 ***g***- and LSCR-grown RF1, RF6 and RF11 cells and cell morphology as determined by scanning and transmission electron microscopy was identical, regardless of the mode of growth (Taylor & Rosado 2007). However, it was clear from visual examination of the cultures that LSCR reduced the amount of staphyloxanthin, the primary yellow staphylococcal pigment strongly linked to virulence (Lui *et al*. 2005). This was confirmed by pigment extraction and quantification and it was further noted that LSCR reduced the haemolytic capacity of culture supernatants, suggesting that modelled microgravity abrogated the secretion of factors linked to staphylococcal virulence (Rosado *et al*. 2010). We therefore investigated the exoproteome of the three isolates under 1 ***g*** and LSCR growth conditions.

As the synthesis of extracellular proteins by *S. aureus* is most apparent during the post-exponential growth phase (Sibbald *et al*. 2006; Jones *et al*. 2008) and cells grew at a slower rate in the HARV, we examined the proteome after 24 hours growth when OD_{600} was approximately 2. Although the exoproteome profiles of 1 ***g***-grown RF1, RF6 and RF11 were broadly comparable, there were clear qualitative and quantitative differences between the strains (Table 2). This observation is consistent with the study of Ziebandt *et al*. (2001) who noted a number of differences in the exoproteome profile of *S. aureus* strains, particularly when clinical isolates were compared

https://doi.org/10.1017/S1473550411000346 Published online by Cambridge University Press

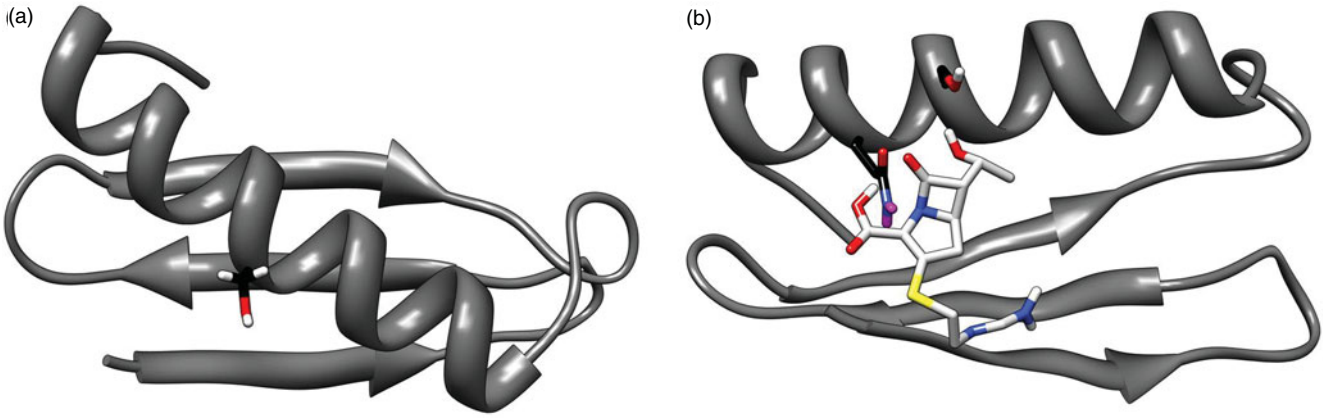


Fig. 4. (a) *Ab initio* structural prediction for VraX showing a conserved serine in the α-helix above and across a plane of two β-sheets. (b) Protein–ligand docking model, which when rotated, suggests a major binding site for the β-lactam imipenem is close to this serine.

(Sibbald *et al*. 2006). There were large differences in the quantity of exoproteins from 1 ***g*** cultures, with RF6 secreting twice that of RF1 and three times that of RF11. These differences were abrogated upon LSCR culture with the exoproteome reduced to a basal level comprising relatively few major components (Fig. 2), the foremost of which was IsaA, one of the few proteins not to be markedly reduced in quantity in the secreted protein fraction (Table 2). In fact, IsaA levels increased significantly under LSCR. This profile shows some similarities with that obtained with *agr* mutants of *S. aureus* RN6390 (Rohl *et al.* 2004) and UAMS-1 (Jones *et al.* 2008): while the abundance of some extracellular, virulence-associated proteins were lower in the *agr* mutants, the amount of IsaA and a limited number of other proteins with potential virulence-enhancing properties were significantly higher. Conversely, IsaA secretion was virtually abolished in a *sarA* mutant of UAMS-1 (Jones *et al.* 2008). IsaA is known to be preferentially produced during exponential phase but present in abundant copy number later in the growth cycle (Jones *et al.* 2008), a profile consistent with its likely role as a lytic transglycosylase involved in peptidoglycan modelling during the growth cycle (Stapleton *et al.* 2007). The expression of the enzyme, present in both the cell wall and secretome (Stapleton *et al.* 2007), is subject to complex regulation and known to be positively regulated by SarA, the two-component sensor–regulator YycFG (Stapleton *et al.* 2007) and SigB (Ziebandt *et al*. 2004); in light of its differential expression in 1 ***g*** and LSCR it is likely that the bulk of the exoproteome modulated by LSCR is under different control processes and our microarray and qRT-PCR data (Table 4) support this contention.

One candidate for a role in the regulation of the LSCR-modulated secretome was the *vraX* gene product: this small polypeptide, identified as a component of the cell wall stress stimulon (Utaida *et al*. 2003), harbours a putative phosphorylation site (Scherl *et al.* 2006) and could therefore be involved in regulatory processes. However, the Δ*vraX* mutant derived from SH1000 did not appear to differ from the wild-type with respect to protein secretion and had no influence on the expression of other staphylococcal genes under the experimental conditions used. We could identify no difference in phenotype as a result of *vraX* gene deletion. However, an *ab initio* protein–ligand docking simulation suggests a major binding site for the β-lactam drug imipenem close to a serine residue in a conserved LLSLL motif found in all VraX homologues that we could identify following an extensive BLAST search. Serine is an essential residue in the catalytic mechanisms of β-lactamases and penicillin-binding proteins. Lysine has also been implicated as the general base involved in the acylation of this serine, although a glutamic acid residue has also been proposed as a candidate for this role (Damblon *et al.* 1996). Given that imipenem binds to VraX, it is intriguing to speculate a role for vraX in the molecular evolution of β-lactamases and other penicillin-binding proteins. Although much is known about the presence and diversity of β-lactamases in staphylococci, surprisingly little is known about how these clinically significant proteins have evolved, which warrants further investigation as a possible alternative route towards the design of novel β-lactamase inhibitors.

Few other candidates with the potential to regulate the LSCR phenotype emerged from the microarray study, although qRT-PCR data suggest that the two-component sensor-regulator SaeRS may be implicated (Table 4). There was in general good accord between microarrays and qRT-PCR for those genes selected for validation although in some cases changes in gene expression reached levels of statistical significance with one technique but not with the other. The changes in gene expression invoked by growth in simulated microgravity were generally small, reflecting the subtle nature of the alterations in the growth environment, and therefore the true significance of these changes needs to be evaluated using other techniques.

Like others (Sibbald *et al*. 2006; Jones *et al*. 2008), we have shown that some proteins with ascribed cytoplasmic functions and without known signals for export can be detected in the extracellular fraction of *S. aureus* cultures. As LSCR partially simulates the microgravity environment by reducing the shear forces to which bacteria in HARV culture are subjected

https://doi.org/10.1017/S1473550411000346 Published online by Cambridge University Press

(Hammond & Hammond 2001), we determined the effect of the growth environment on release of DNA into the growth medium at the time of cell harvest; we could find no evidence for a significant decrease in cell lysis due to LSCR by TEM, SEM (Taylor & Rosado 2007; Rosado *et al.* 2010) or DNA release profiling, nor was there any reduction in OD_{600} during growth under LSCR. Although some of the proteins we detected are among the most abundant in the cytoplasm, there is evidence that some glycolytic enzymes are specifically exported into the growth medium by incompletely defined processes (Boël *et al*. 2004). Further, the differential modulation of the exoproteome by LSCR over the 1 ***g*** phenotype (Fig. 3) is unlikely to occur through processes involving changes in cell lytic activity alone.

The broad similarity in the gene expression profiles encountered when *S. enterica* was cultured in the HARV (Wilson *et al*. 2002) and aboard Space Shuttle mission STS-115 (Wilson *et al*. 2007) has led to the suggestion of a microgravity regulon, with differential regulation of a large number of genes involved in diverse functional groups. We found no evidence for such wholesale recalibration of cellular activity but we have examined a simulation of only one component of the reduced gravity environment. As *S. aureus* may pose a risk to crew well being during extended space flight, the impact of reduced gravity, as well as other factors relevant to flight such as acceleration, vibration, radiation and electromagnetism, should be evaluated in space and the recent completion of the ISS could provide an opportunity to undertake such experiments over extended periods of time.

Acknowledgements

The study was supported by a grant from Fundação para a Ciência e a Tecnologia, Portugal.

Author disclosure statement

No competing financial interests exist.

References

Bae, T. & Schneewind, O. (2006). *Plasmid* **55**, 58–63.
Benoit, M. & Klaus, D.M. (2007). *Adv. Space Res*. **39**, 1225–1232.
Bernal, P., Lemaire, S., Pinho, M.G., Mobashery, S., Hinds, J. & Taylor, P.W. (2010). *J. Biol. Chem*. **285**, 24055–24065.
Boël, G., Pichereau, V., Mijakovic, I., Mazé, A., Poncet, S., Gillet, S., Giard, J.-C., Hartke, A., Auffray, Y. & Deutscher, J. (2004). *J. Mol. Biol*. **337**, 485–496.
Damblon, C., Raquet, X., Lian, L.Y., Lamotte-Brasseur, J., Fonze, E., Charlier, P., Roberts, G.C. & Frère, J.M. (1996). *Proc. Natl. Acad. Sci. USA* **93**, 1747–1752.
Du, B., Daniels, V.R., Vaksman, Z., Boyd, J.L., Crady, C. & Putcha, L. (2011). *AAPS J*. **13**, 299–308.
Giraudo, A.T., Cheung, A.L. & Nagel, R. (1997). *Arch. Microbiol*. **168**, 53–58.
Hammond, T.G. & Hammond, J.M. (2001). *Am. J. Physiol. Renal Physiol*. **281**, 12–25.
Horsburgh, M.J., Aish, J.L., White, I.J., Shaw, L., Lithgow, J.K. & Foster, S.J. (2002). *J. Bacteriol*. **184**, 5457–5467.
Jones, R.C., Deck, J., Edmondson, R.D. & Hart, M.E. (2008). *J. Bacteriol*. **190**, 5265–5278.
Juergensmeyer, M.A., Juergensmeyer, E.A. & Guikema, J.A. (1999). *Micrograv. Sci. Technol*. **12**, 41–47.
Klaus, D.M. (2002). In *Encyclopedia of Environmental Microbiology*, ed. Britton, G., pp. 2996–3004. John Wiley and Sons, New York.
Lapchine, L., Moatti, N., Gasset, G., Richoilley, G., Templier, J. & Tixador, R. (1985). *Drugs Exp. Clin. Res*. **12**, 933–938.
Leaver-Fay, A., Tyka, M., Lewis, S.M., Lange, O.F., Thompson, J., Jacak, R., Kaufman, K., Renfrew, P.D., Smith, C.A., Sheffler, W. *et al.* (2011). *Methods Enzymol*. **487**, 545–574.
Lui, G.Y., Essex, A., Buchanan, J.T., Datta, V., Hoffman, H.M., Bastian, J.F., Fierer, J. & Nizet, V. (2005). *J. Exp. Med*. **202**, 209–215.
McAleese, F., Wu, S.W., Sieradzki, K., Dunman, P., Murphy, E., Projan, S. & Tomasz, A. (2006). *J. Bacteriol*. **188**, 1120–1133.
Morris, G.M., Huey, R., Lindstrom, W., Sanner, M.F., Belew, R.K., Goodsell, D.S. & Olson, A.J. (2009). *J. Comput. Chem*. **30**, 2785–2791.
Muthaiyan, A., Silverman, J.A., Jayaswal, R.K. & Wilkinson, B.J. (2008). *Antimicrob. Agents Chemother*. **52**, 980–990.
Nauman, E.A., Ott, C.M., Sander, E., Tucker, D.L., Pierson, D., Wilson, J.W. & Nickerson, C.A. (2007). *Appl. Environ. Microbiol*. **73**, 699–705.
Nickerson, C.A., Ott, C.M., Mister, S.J., Morrow, B.J., Burns-Keliher, L. & Pierson, D.L., (2000). *Infect. Immun*. **68**, 3147–3152.
Nickerson, C.A., Ott, C.M., Wilson, J.W., Ramamurthy, R., LeBlanc, L., Höner zu Bentrup, K., Hammond, T. & Pierson, D.L. (2000). *J. Microbiol. Meth*. **54**, 1–11.
Nickerson, C.A., Ott, C.M., Wilson, J.W., Ramamurthy, R. & Pierson, D.L. (2004). *Microbiol. Mol. Biol. Rev*. **68**, 345–361.
Novick, R.P. (2003). *Mol. Microbiol*. **48**, 1429–1449.
Novick, R.P. & Jiang, D. (2003). *Microbiology* **149**, 2709–2717.
Novikova, N. (2004). *Microbiol. Ecol*. **47**, 127–132.
Novikova, N., De Boever, P., Poddubko, S., Deshevaya, E., Polikarpov, N., Rakova, N., Coninx, I. & Mergeay, M. (2006). *Res. Microbiol*. **157**, 5–12.
O'Neill, A.J. (2010). *Lett. Appl. Microbiol*. **51**, 358–361.
Rohl, C.A., Strauss, C.E., Misura, K.M. & Baker, D. (2004). *Methods Enzymol*. **383**, 66–93.
Rosado, H., Doyle, M., Hinds, J. & Taylor, P.W. (2010). *Acta Astronaut*. **66**, 408–413.
Scherl, A., François, P., Charbonnier, Y., Deshusses, J.M., Koessler, T., Huyghe, A., Bento, M., Stahl-Zeng, J., Fischer, A., Masselot, A. *et al.* (2006). *BMC Genom*. **7**, 296.
Schwartz, R.P., Goodwin, T.J. & Wolf, D.A. (1992). *J. Tiss. Cult. Meth*. **14**, 51–58.
Sibbald, M.J.J.B., Ziebandt, A.K., Engelmann, S., Hecker, M., de Jong, A., Harmsen, H.J.M., Raangs, G.C., Stokroos, I., Arends, J.P., Dubois, J.Y.F. *et al.* (2006). *Microbiol. Mol. Biol. Rev*. **70**, 755–788.
Sonnenfeld, G. (2005). *Curr. Pharm. Biotechnol*. **6**, 343–349.
Sonnenfeld, G. & Shearer, W.T. (2002). *Nutrition* **18**, 899–903.
Stapleton, M.R., Horsburgh, M.J., Hayhurst, E.J., Wright, L., Jonsson, I.-M., Tarkowski, A., Kokai-Kun, J.F., Mond, J.J. & Foster, S.J. (2007). *J. Bacteriol*. **189**, 7316–7325.
Taylor, G.R. (1974). *Aerospace Med*. **45**, 824–882.
Taylor, P.W. & Rosado, H. (2007). *Planet Mars Research Focus*, ed. Costas L.A., pp. 165–185. Nova Science, Hauppauge, NY.
Tixador, R., Richoilley, G., Gasset, G., Templier, J., Bes, J.C., M'oatti, N. & Lapchine, L. (1985). *Aviat. Space Environ. Med*. **56**, 748–751.
Tjalsma, H., Anteman, H., Jongbloed, J.D.H., Braun, P.G., Darmon, E., Dorenbos, R., Dubois, J.-Y.F., Westers, H., Zanen, G., Quax, W.J. *et al.* (2004). *Microbiol. Mol. Biol. Rev*. **68**, 207–233.
Utaida, S., Dunman, P.M., Macapagal, D., Murphy, E., Projan, S.J., Singh, V.K., Jayaswal, R.K. & Wilkinson, B.J. (2003). *Microbiology* **149**, 2719–2732.
Wilson, J.W., Ramamurthy, R., Porwollick, S., McClelland, M., Hammond, T., Allen, P., Ott, C.M., Pierson, D.L. & Nickerson, C.A. (2002). *Proc. Natl. Acad. Sci. U.S.A.* **99**, 13807–13812.

https://doi.org/10.1017/S1473550411000346 Published online by Cambridge University Press

Wilson, J.W., Ott, C.M., Höner zu Bentrup, K., Ramamurthy, R., Quick, L., Porwollik, S., Cheng, P., McClelland, M., Tsaprailis, G., Radabaugh, T. *et al.* (2007). *Proc. Natl. Acad. Sci. U.S.A.* **104**, 16299–16304.

Wilson, J.W., Ott, C.M., Quick, L., Davis, R., Höner zu Bentrup, K., Crabbé, A., Richter, E., Sarker, S., Barrila, J., Porwollik, S. *et al.* (2008). *PLoS ONE* **3**, e3923.

Witney, A.A., Marsden, G.L., Holden, M.T., Stabler, R.A., Husain, S.E., Vass, J.K., Butcher, P.D., Hinds, J. & Lindsay, J.A. (2005). *Appl. Environ. Microbiol.* **71**, 7504–7514.

Ziebandt, A.K., Becher, D., Ohlsen, K., Hacker, J., Hecker, M. & Engelmann, S. (2004). *Proteomics* **4**, 3034–3047.

Ziebandt, A.K., Weber, H., Rudolph, J., Schmid, R., Hoper, D., Engelmann, S. & Hecker, M. (2001). *Proteomics* **1**, 480–493.

https://doi.org/10.1017/S1473550411000346 Published online by Cambridge University Press